Accuracy of molecular data in the understanding of ultracold collisions

O. Dulieu
Laboratoire des Collisions Atomiques et Moléculaires, Bâtiment 351, Université Paris-Sud, 91405 Orsay Cedex, France

P. Julienne
Molecular Physics Division, National Institute of Standards and Technology, Gaithersburg, Maryland 20899

J. Weiner
Department of Chemistry and Biochemistry, University of Maryland, College Park, Maryland 20742
(Received 14 June 1993)

We show through close-coupled quantum-scattering calculations that the cross section for fine-structure-changing collisions between excited $^2P_{3/2}$ and ground $^2S_{1/2}$ A atoms of the same species, where A = Rb or Cs, is very sensitive to the molecular potentials and spin-orbit matrix elements of the alkali-metal-dimer species. Spectroscopic studies of these species are needed to extract accurate parameters. New high-resolution photoassociation spectroscopy of trapped atoms could be used for this purpose.

PACS number(s): 32.80.Pj

Recent ultracold collision experiments have demonstrated novel physical features which have opened an entirely new research field [1–16]. In this collision regime an extreme sensitivity to long-range potentials as well as photon absorption and spontaneous decay during the collision process constitute important issues that require critical examination. This Brief Report considers some aspects of this ultracold regime that challenges theoretical calculation of inelastic rate constants. Due to the presence of both excited- and ground-state atoms, fine-structure- (FS) changing collisions between alkali-metal atoms,

$$A(^2P_{3/2})+A \rightarrow A(^2P_{1/2})+A \ , \quad A=\mathrm{Rb,Cs} \ , \tag{1}$$

and the radiative-escape (RE) process

$$A(^2P_{3/2})+A(^2S) \rightarrow A(^2S,\mathrm{fast})+A(^2S,\mathrm{fast})+h\nu \ , \quad A=\mathrm{Rb,Cs} \ , \tag{2}$$

contribute principally to trap loss rate [3–5], [7–9]. In this Brief Report, we illustrate in process (1) the role of the *decreasing number of partial waves* of the nuclear motion as collision energy decreases to the ultracold regime. We find a dramatic sensitivity of the calculated rate constant due to three factors: (i) the isotopic difference in the mass of the collision partners, (ii) the accuracy of molecular spin-orbit coupling, and (iii) the accuracy of molecular potential curves, especially on the short-range repulsive branch. Recent experiments in magneto-optical traps (MOT's) [15,16] exhibit high-resolution molecular photoassociation spectra which may provide new opportunities for extracting needed spectroscopic data.

An ultracold collision divides into inner and outer zones [13] with specific physical characteristics. The *outer zone* begins around $R=R_v$, where the molecular potential (proportional to $1/R^3$ for a $S+P$ collision) shifts about one natural linewidth below the asymptotic energy. For alkali atoms, this region begins at about $R_v=2000a_0$ ($1a_0=5.291\,77\times10^{-11}$ m is the Bohr radius of the hydrogen atom). At internuclear distances closer than this point the $(S+P)$ molecular system is no longer in resonance with an excitation laser tuned one linewidth from resonance, and might emit spontaneously before reaching the *inner zone* (typically below $R_{\mathrm{in}}\approx100a_0$) where strong molecular interactions may induce a FS transition.

For an $(S+P)$ ultracold collision at energy E and corresponding relative velocity v, the rate constant may be generally expressed [13]:

$$K=\frac{1}{2g_1g_2}\frac{\pi v}{k_\infty^2}\sum_{N=0}^{N_{\max}}(2N+1)P_x(E,N) \times P_{\mathrm{in}}(E,R_{\mathrm{in}},N,\delta,I) \ , \quad x=\mathrm{FS\ or\ RE} \ . \tag{3}$$

The initial kinetic energy in the entrance channel is given by $E=\hbar k_\infty^2/2\mu$, where μ is the reduced mass, and g_1 and g_2 are the atomic degeneracies in the $^2S_{1/2}$ and $^2P_{1/2}$ states. The sum over N is limited to the number $N_{\max}$ of partial waves of the nuclear motion up to the centrifugal barrier cutoff. The probability for the x process to occur in the inner zone is P_x. The probability P_{in}, depending on the laser power I and detuning δ from the resonant atomic excitation, reflects the unique ultracold effects, i.e., the probability for the excited system to reach the internal reaction zone after excitation at very large R. When the temperature $T=E/k_B$ is lower than a characteristic temperature for which the excited atom spontaneous decay time is comparable to the collision time, P_{in} depends on complicated collision dynamics associated with excited-state decay and hyperfine structure. Approximate local equilibrium [13] and semiquantal optical Bloch equation [14] models have been proposed to calcu-

late $P_{\rm in}$, but these issues are beyond the scope of the present paper. Ultimately, fully quantal calculations with dissipation and hyperfine structure are required to calculate $P_{\rm in}$ correctly. Recent experiments have demonstrated the strong influence of hyperfine couplings on the ultracold dynamics [3,4,6,7]. We ignore hyperfine structure here since it is unlikely to have any significant effect on P_x.

In the following we shall discuss only the $x=$FS process. We focus on the evaluation of the probability $P_{\rm FS}$ and the corresponding quantum opacity $\sigma(E)$ calculated for the internal region

$$\sigma(E)=\sum_{N=0}^{N_{\max}}(2N+1)P_{\rm FS}(E,N)\ . \tag{4}$$

We have performed quantum close-coupling calculations within a total angular-momentum representation in which the electronic-rotational Hamiltonian is asymptotically diagonal. There are six coupled channels for each set of quantum numbers (J,π,p_e), where J is the total (i.e., electronic + rotational) angular momentum, π the *gerade* (g) or *ungerade* (u) parity, and p_e the parity e or f associated with the total angular-momentum states [17]. We have used the new accurate Born-Oppenheimer potential curves of Foucrault, Daudey, and Millié [18], for Rb_2 and Cs_2 instead of model curves used in previous calculations [13]. A matrix transformation [19] yields the connection between the Hamiltonian in molecule- and space-fixed quantization schemes.

Typical alkali-metal Born-Oppenheimer u potential curves dissociating to the first $ns+np$ limit are shown in Fig. 1(a). The main feature is the crossing between $A\,^1\Sigma_u^+$ and $b\,^3\Pi_u$ states at short-range $R=R_{\rm SR}$ ($\approx 9.5a_0$ in Rb_2, $\approx 10.5a_0$ in Cs_2). Four other g curves exist but are not drawn, as it has been well established that the g manifold does not contribute significantly to the process [20]. Diagonalizing the electronic + fine-structure Hamiltonian gives the adiabatic potentials shown in Fig. 1(b). There are only two attractive entrance channels for process (1), 0_u^+ and 2_u which correlate to the $^2S_{1/2}+{}^2P_{3/2}$ limit. Another crossing occurs at $R=R_{\rm LR}$ between this 0_u^+ state and the attractive 1_u state correlated to the $^2S_{1/2}+{}^2P_{1/2}$ limit ($\approx 23.5a_0$ in Rb_2, $\approx 17.5a_0$ in Cs_2).

There are three basic mechanisms for FS transitions [21]: (FS1) spin-orbit interaction leading to the transition between the $A\,^1\Sigma_u^+$ and $b\,^3\Pi_u$ states around their short-range crossing, (FS2) Coriolis mixing of the three fine-structure components of the $b\,^3\Pi_u$ state, and (FS3) Coriolis coupling between the 0_u^+ and 1_u states at their long-range crossing. The FS1 process is dominant for heavy alkali dimers Cs_2 and Rb_2, while Coriolis coupling (FS2 and FS3) yields the major contribution in Na_2. Following Ref. [13], the molecular spin-orbit operator $V_{\rm so}$ responsible for the transition at the inner crossing point for Cs_2 and Rb_2 is approximately scaled to the experimental data for Li_2, Na_2, and K_2.

We will illustrate our discussion with the two isotopes of rubidium, but we find similar results for cesium. The *six-channel* quantum probabilities $P_{\rm FS}$ as a function of angular-momentum quantum number N are plotted in Figs. 2(a) and 2(b) at $T=50$ K and 1 mK, respectively. In Fig. 2(a), we see usual Stückelberg quantum oscillations up to a cutoff determined by the height of the long-range centrifugal barrier, around $N_{\max}=350$. Computed cross sections are very similar for both isotopes: $299a_0^2$ for ^{85}Rb, $290a_0^2$ for ^{87}Rb. At initial temperatures, low compared to the well depth of the potential curves ($\approx 4000\ {\rm cm}^{-1}$ or ≈ 5750 K), the probability $P_{\rm FS}(E,N)$ is insensitive to collision energy and $\sigma(E)$ is essentially determined by the position of the centrifugal barrier cutoff $N_{\max}$. For 1 mK the cutoff occurs at $N_{\max}=53$. As shown in Fig. 2(b), only a fraction of a quantum oscillation will contribute to $P_{\rm FS}$. In contrast to Fig. 2(a), $\sigma(E)$ is no longer an average over many oscillations. The value of $P_{\rm FS}(E,0)$ is strongly affected by the mass difference between the two isotopes, and therefore the opacities $\sigma(E)$ calculated for the two curves in Fig. 2(b) differ by about one order of magnitude.

The familiar semiclassical Landau-Zener model allows a qualitative explanation of this *kinetic* effect. Introducing Stüeckelberg interference terms in the semiclassical probability associated with the short-range crossing point $R_{\rm SR}$ between the $A\,^1\Sigma_u^+$ and $b\,^2\Pi_u$ curves, we have [22]

$$P_{\rm FS}^{\rm LZS}(N)=2p_N(1-p_N)2\sin^2\delta_N\ , \tag{5}$$

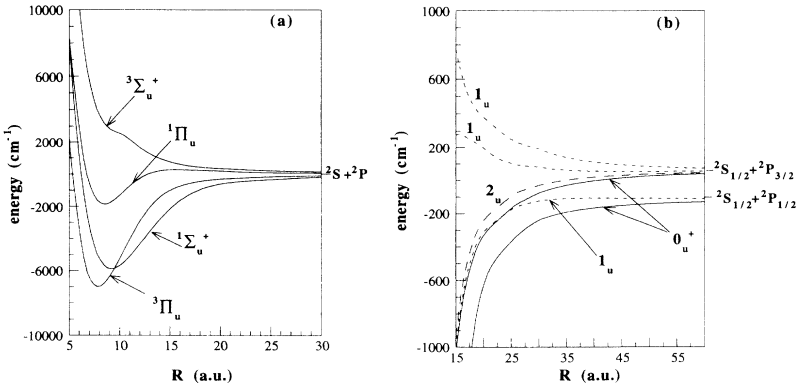

FIG. 1. Typical potential curves for an alkali-metal dimer (Rb_2) correlated to $^2S+{}^2P$ dissociation limit: (a) without fine structure; (b) including fine structure.

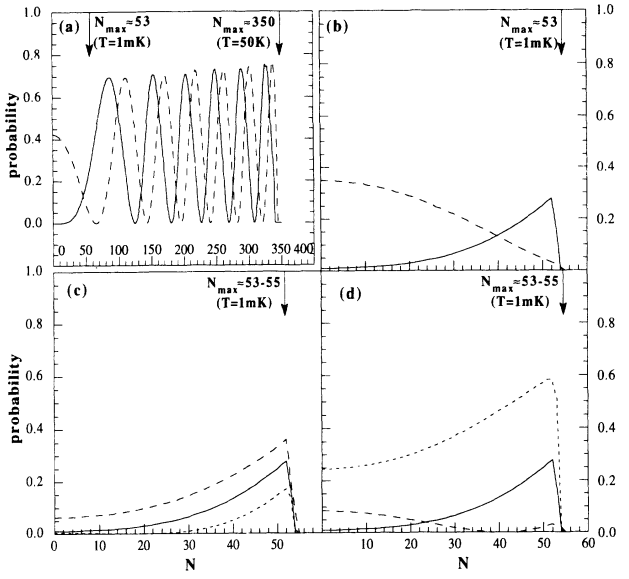

FIG. 2. FS transition probability for a Rb(^2S)-Rb(^2P) collision as a function of partial wave N. (a) At $T=50$ K. Full line, ^{85}Rb isotope; dashed line, ^{87}Rb isotope. The position of the cutoff N_{max} is indicated for $T=50$ K and 1 mK. (b) Same as (a) at $T=1$ mK. (c) At $T=1$ mK, for ^{85}Rb. Full line, $V_{so}=81$ cm^{-1}; dashed line, $V_{so}=73$ cm^{-1}; short-dashed line, $V_{so}=89$ cm^{-1}. (d) At $T=1$ mK, for ^{85}Rb. Full line, $R_t=5.34a_0$; dashed line, $R_t=5.35a_0$; short-dashed line, $R_t=5.33a_0$.

where p_N is the well-known single-crossing Landau-Zener transition probability at R_{SR}. The phase δ_N is the difference of classical action between the two molecular paths $A\,^1\Sigma_u^+$ and $b\,^3\Pi_u$:

$$\delta_N=\int_{R_t^{(1)}}^{R_c}k_N^{(1)}(R)dR-\int_{R_t^{(2)}}^{R_c}k_N^{(2)}(R)dR\ , \tag{6}$$

where

$$k_n^{(i)}(R)=\left[\frac{2\mu}{\hbar^2}\left[E-V^{(i)}(R)-\frac{N(N+1)}{2\mu R^2}\right]\right]^{1/2} \tag{7}$$

is the local wave number at distance R in channel (i), for each partial-wave N. Due to the large well depths, the classical action in each channel reaches very large values, leading also to large values for δ_N. The phase δ_N is proportional to $\sqrt{\mu}$ and changes from 76 to 76.75 rad between the lighter and the heavier isotope. This mass variation of $\sqrt{(87-85)/85}=1.5\%$ produces a phase shift of about $\pi/4$ rad in δ_N, resulting in a pronounced change in the oscillatory factor in Eq. (5). From Eq. (7), we see that δ_N depends on $V^{(i)}(R)$ as well as on μ. Therefore the accuracy of molecular parameters introduced into our model has to be checked carefully before interpreting P_{FS} in terms of a large mass effect.

In Cs_2 and Rb_2, the *molecular* spin-orbit operator V_{so} responsible for the transition at the inner crossing point may be approximately scaled to the experimental data for Li_2, Na_2, and K_2. This leads to the *R-independent* value [13] $V_{so}=0.34\ \Delta E_{FS}=81$ cm^{-1} for Rb_2, where ΔE_{FS} is the atomic fine-structure splitting. However, this procedure does not guarantee an accuracy for V_{so} better than $\pm 10\%$. In Fig. 2(c), we have plotted the probability P_{FS} at $T=1$ mK, for three values of V_{so} within the above range: 73, 81, and 89 cm^{-1}. This uncertainty results in a shift in the potentials with a consequent change in δ_N in Eq. (6), while having a negligible effect on p_N. The calculated opacity $\sigma(E)$ varies by a factor of 4 over these three cases, corresponding to a variation of $\approx 0.5\%$ of δ_N. The present scaling of V_{so} is therefore too approximate for reliable comparison to the experiment. A better knowledge of V_{so} is particularly required for the heavy alkali dimers, *both in magnitude and variation with internuclear distance.*

Another major uncertainty arises from the determination of the molecular potentials themselves. In Rb_2 and Cs_2, the spin-orbit interaction between $A\,^1\Sigma_u^+$ and $b\,^3\Pi_u$ states is strong enough to perturb their vibrational spectrum for high v levels and their potential curves have been determined spectroscopically only in the vicinity of their minimum. Therefore, the best we can do is to use the most accurate available quantum-chemical calculations [18]. Their uncertainty is about 50 cm^{-1} or $\approx 1\%$ of the well depth, and induces the same uncertainty in δ_N as the mass effect. The consequences for $P_{FS}(N)$ are the same: varying the potential curves within this accuracy range leads again to very different $P_{FS}(N)$ and the deduced opacity will not be meaningful. However, even if accurate spectroscopic determination of these curves were available over a wide range of internuclear distances, the position of the inner classical turning point of the highest vibrational levels in the excited-state potentials will remain uncertain. Quantum-chemical methods lose accuracy in the corresponding range of internuclear distances ($R<6a_0$). One is forced to extrapolate somewhat arbitrarily the repulsive part of the potential curve used in the calculations. Figure 2(d) plots P_{FS} for three plausible exponential extrapolations from the last calculated point ($R=6a_0$, ≈ 3000 cm^{-1} below the dissociation limit) of the $b\,^3\Pi_u$ curve, yielding a turning point of the last vibrational level at $R_t=5.34\pm 0.01a_0$. Due to the deep potential well and the consequent large value of $k_N^{(i)}$, the phase δ_N varies by an amount of about 1% over these three cases, again resulting in an order of magnitude variation in the calculated opacity.

The question of comparison to experimental results must be addressed. Recent results [4,7] in a rubidium MOT show a significant difference between the two isotopes in the dependence of the trap-loss rate constant to the detuning of the trapping laser. At large detunings ($\delta>300$ MHz), the rate constants are almost identical within the experimental error bars. At small detunings, the rate constant is measured to be three to four times larger for ^{85}Rb - ^{85}Rb collisions than for ^{87}Rb - ^{87}Rb collisions. The mass sensitivity described in our calculations affects only the probability P_{FS}, and is not expected to be important for P_{RE}. Application of the theory in Ref. [13] shows that P_{FS} and P_{RE} have comparable magnitudes at large detunings, thereby attenuating the contribution of the mass effect to the total trap-loss rate. In contrast, the FS process dominates at small detunings, consistent with

the possibility of a significant mass effect. A complete understanding of these processes requires not only very accurate molecular data but also a treatment of the dynamical role of the hyperfine structure.

Finally, the realization of high-resolution photoassociation spectroscopy in very recent experiments [15,16] on ultracold trapped atoms offers new prospects for experimental studies of molecular potentials near a dissociation limit. Reference [13] pointed out that resolved bound-state spectra could be used to measure the near-threshold opacity directly from the predissociation linewidths of bound molecular states lying between the molecular-dissociation limits. The same mechanism that leads to the FS collision leads to bound-state predissociation. Therefore, photoassociation spectroscopy of the 0_u^+ state (which is optically active at long range) could in principle measure $P_x(E_v, N=0, 0_u^+)$ directly. Standard spectroscopic analysis of measured bound-state energies could be used to refine the potentials to permit much more accurate calculations.

The authors would like to thank Ph. Millié for providing us with his numerical potential curves, and to E. E. Nikitin and E. I. Dashevskaya for stimulating discussions. This work has been supported in part by a joint international cooperation between CNRS and NSF. One of us (P.S.J.) would like to thank the Université Paris–Sud for supporting his visit at Laboratoire des Collisions Atomiques et Moléculaires. The Laboratoire des Collisions Atomiques et Moléculaires is "Unité No. UA0281 au CNRS."

[1] P. L. Gould, P. D. Lett, P. S. Julienne, W. D. Phillips, H. R. Thorsheim, and J. Weiner, Phys. Rev. Lett. **60**, 788 (1988).

[2] P. D. Lett, P. S. Jessen, W. D. Philips, S. L. Rolston, C. I. Westbrook, and P. L. Gould, Phys. Rev. Lett. **67**, 2139 (1991).

[3] M. Wagshul, K. Helmerson, P. D. Lett, S. L. Rolston, W. D. Phillips, R. Heather, and P. S. Julienne, Phys. Rev. Lett. **70**, 2074 (1993).

[4] C. D. Wallace, T. P. Dinneen, K.-Y. T. Yan, T. T. Grove, and P. L. Gould, Phys. Rev. Lett. **69**, 897 (1992).

[5] L. Marcassa, V. Bagnato, Y. Wang, C. Tsao, J. Weiner, O. Dulieu, Y. B. Band, and P. S. Julienne, Phys. Rev. A **47**, 4563 (1993).

[6] V. Bagnato, L. Marcassa, Y. Wang, and J. Weiner, Phys. Rev. Lett. **70**, 3225 (1993).

[7] P. Feng, D. Hoffman, and T. Walker, Phys. Rev. A **47**, R3495 (1993).

[8] D. Sesko, T.Walker, C. Monroe, A. Gallagher, and C. Wieman, Phys. Rev. Lett. **63**, 961 (1989).

[9] D. Hoffman, P. Feng, R. S. Williamson III, and T. Walker, Phys. Rev. Lett. **69**, 753 (1992).

[10] P. S. Julienne and R. Heather, Phys. Rev. Lett. **67**, 2135 (1991).

[11] H. R. Thorsheim, Y. Wang, and J. Weiner, Phys. Rev. A **41**, 2873 (1990).

[12] Y. Wang and J. Weiner, Phys. Rev. A **42**, 675 (1990); and (unpublished) results.

[13] P. Julienne and J. Vigué, Phys. Rev. A **44**, 4464 (1991).

[14] Y. B. Band and P. S. Julienne, Phys. Rev. A **46**, 330 (1992).

[15] P. D. Lett, S. L. Rolston, P. S. Jessen, K. Helmerson, M. Wagshul, W. D. Phillips, and L. P. Ratliff, Phys. Rev. Lett. **71**, 2200 (1993).

[16] D. Heinsen (private communication).

[17] R. L. Dubs and P. S. Julienne, J. Chem. Phys. **95**, 4177 (1991).

[18] M. Foucrault, J. P. Daudey, and Ph. Millié, J. Chem. Phys. **96**, 1257 (1992).

[19] B. Pouilly and M. H. Alexander, J. Chem. Phys. **86**, 4790 (1987).

[20] E. I. Dashevskaia, A. I. Voronin, and E. E. Nikitin, Can. J. Phys. **47**, 1237 (1969).

[21] E. I. Dashevskaia, Opt. Spektrosk. **46**, 423 (1979) [Opt. Spectrosc. **46**, 236 (1979)].

[22] See, for example, N. F. Mott and H. S. W. Massey, *The Theory of Atomic Collisions,* 3rd ed. (Oxford University Press, London, 1965).